The human placenta methylome

Diane I. Schroeder[a,b,c], John D. Blair[d], Paul Lott[b], Hung On Ken Yu[b], Danna Hong[a], Florence Crary[a,b,c], Paul Ashwood[a,c,e], Cheryl Walker[c,f], Ian Korf[b], Wendy P. Robinson[d], and Janine M. LaSalle[a,b,c,1]

[a]Department of Medical Microbiology and Immunology, UC Davis School of Medicine, Davis, CA 95616; [b]UC Davis Genome Center, University of California, Davis, CA 95616; [c]UC Davis MIND Institute, University of California Davis, Sacramento, CA 95817; [d]Department of Medical Genetics, University of British Columbia, Vancouver, BC, Canada V5Z 4H4; [e]Center for Children's Environmental Health Sciences, UC Davis School of Medicine, Sacramento, CA 95817; and [f]Department of Obstetrics and Gynecology, UC Davis School of Medicine, Sacramento, CA 95817

Edited by Jasper Rine, University of California, Berkeley, CA, and approved March 4, 2013 (received for review September 4, 2012)

Tissue-specific DNA methylation is found at promoters, enhancers, and CpG islands but also over larger genomic regions. In most human tissues, the vast majority of the genome is highly methylated (>70%). Recently, sequencing of bisulfite-treated DNA (MethylC-seq) has revealed large partially methylated domains (PMDs) in some human cell lines. PMDs cover up to 40% of the genome and are associated with gene repression and inactive chromatin marks. However, to date, only cultured cells and cancers have shown evidence for PMDs. Here, we performed MethylC-seq in full-term human placenta and demonstrate it is the first known normal tissue showing clear evidence of PMDs. We found that PMDs cover 37% of the placental genome, are stable throughout gestation and between individuals, and can be observed with lower sensitivity in Illumina 450K Infinium data. RNA-seq analysis confirmed that genes in PMDs are repressed in placenta. Using a hidden Markov model to map placental PMDs genome-wide and compare them to PMDs in other cell lines, we found that genes within placental PMDs have tissue-specific functions. For regulatory regions, methylation levels in promoter CpG islands are actually higher for genes within placental PMDs, despite the lower overall methylation of surrounding regions. Similar to PMDs, polycomb-regulated regions are hypomethylated but smaller and distinct from PMDs, with some being hypermethylated in placenta compared with other tissues. These results suggest that PMDs are a developmentally dynamic feature of the methylome that are relevant for understanding both normal development and cancer and may be of use as epigenetic biomarkers.

epigenomics | hypomethylation

It has long been known that most human tissues have high levels of DNA methylation genome-wide (1). Other tissues, such as placenta and some cancers, have lower levels of methylation (2) but little was known about how the hypomethylated DNA was organized within the genome. Recent genome-wide DNA methylation sequencing studies have shown that some hypomethylated genomes, such as mouse maturing red blood cells and human adipose-derived stem cells, have lower methylation genome-wide (3, 4). However, an interesting subset of hypomethylated cells were recently found to have lower methylation only in large partially methylated domains (PMDs), which are distinct from the surrounding highly methylated domains (HMDs) (5, 6). In these cells, PMDs can cover as much as 40% of the genome and tend to be over 100 kb in length. Genes in PMDs are usually repressed and have tissue-specific functions unrelated to the tissue of origin. For example, when comparing the PMD distributions in human IMR90 fetal lung fibroblasts and SH-SY5Y neuroblastoma cells, genes that were in PMDs in IMR90 cells but in HMDs in SH-SY5Y cells had synaptic transmission and neuron differentiation functions (6). In contrast, genes in PMDs in SH-SY5Y cells but in HMDs in IMR90 cells had respiratory tube development functions. These epigenetic differences suggest that the localization of genes within PMDs may play a role in their repression during normal human tissue development. In addition, PMDs may explain the global hypomethylation observed in some cancers as some colon (7, 8) and breast cancers (9, 10) have PMDs that cover large portions of the genome.

To date, PMDs have been observed in cultured cells but not in normal human tissue. Human placenta is known to have lower levels of global DNA methylation (1, 11–13) but whether placental tissue shows lower methylation genome-wide or has PMDs is currently unknown since many studies focus on promoters, CpG islands, and repetitive elements (14). A few locus-specific microarray-based studies have found that genes with higher tissue-specific expression in placenta also have higher DNA methylation in their gene bodies (15, 16). In addition, Chu et al. (15) found large regions of hypomethylation in placenta compared with maternal blood cells; however, the analysis was limited to chromosomes 13,18, and 21. Further study of DNA methylation in placenta is warranted because changes in placental methylation have been associated with infant growth rate, pre-eclampsia, and preterm delivery (17–21). Furthermore, the placenta is the key mediator of environmental exposures affecting developmental programming of the fetus, which can have long-lasting effects on health (22).

In addition to PMDs, local regions of hypomethylation can also occur over polycomb-regulated genes. Unmethylated CpG islands are able to recruit polycomb complexes (23–25) and because polycomb-regulated regions tend to have clusters of hyperconserved CpG islands (26–28), this can create extended regions of hypomethylation. These hypomethylated regions have been called "methylation deserts" (29) and are enriched for transcription factors involved in development such as the homeobox (HOX) gene clusters. However, the extent that PMDs and polycomb-regulated regions are related is unknown.

This study used a whole genome direct sequencing of bisulfite treated DNA (MethylC-seq) approach as well as Illumina Infinium 450K arrays. Our results demonstrate that placenta is a non-cultured human tissue that exhibits strong evidence for PMDs. These PMDs are stable across placental samples and developmental time points, are distinct from polycomb hypomethylation, and cover tissue-specific genes.

Results

Human Placenta Contains PMDs That Cover Repressed, Tissue-Specific Developmental Genes. To determine the methylomic landscape of human placental tissue, we isolated DNA from chorionic villi sampled from the fetal side of a full term male delivery to avoid

Author contributions: D.I.S. and J.M.L. designed research; D.I.S., J.D.B., D.H., and F.C. performed research; J.D.B., P.L., P.A., C.W., I.K., and W.P.R. contributed new reagents/analytic tools; D.I.S., P.L., and H.O.K.Y. analyzed data; and D.I.S. and J.M.L. wrote the paper.

The authors declare no conflict of interest.

Data deposition: The MethylC-seq and RNA-seq data reported in this paper have been deposited in the Gene Expression Omnibus (GEO) database, www.ncbi.nlm.nih.gov/geo (accession nos. GSE39776, GSE39775, GSE32268, and GSE25930). The Illumina 450K data reported in this paper have been deposited in the GEO database, www.ncbi.nlm.nih.gov/geo (accession no. GSE42409), and the ArrayExpress database, www.ebi.ac.uk/arrayexpress (accession no. E-MTAB-1508).

[1]To whom correspondence should be addressed. E-mail: jmlasalle@ucdavis.edu.

This article contains supporting information online at www.pnas.org/lookup/suppl/doi:10.1073/pnas.1215145110/-/DCSupplemental.

GENETICS

any contamination with maternal tissue (i.e., decidua) (12). DNA isolation and bisulfite conversion were performed on two technical replicates from the same placenta. A total of 55 million 85 bp reads were of high quality and uniquely mapped to the genome, generating an average 1.6× genome coverage, a depth we previously showed to be sufficient for detecting large-scale PMDs (6). Bisulfite conversion efficiency (as determined using the percentage of non-CpG cytosines that were unconverted) was 99.3%. The technical replicates had an average of 62.44% and 63.39% methylation over all CpG sites, respectively. Use of a running mean average of k = 9 CpG sites gave a Spearman correlation of 0.81 (Fig. S1 *A* and *B*), suggesting that local average methylation levels are very similar between the two replicates.

For comparison, DNA samples were isolated from three different postmortem human tissues: cerebellum (from an 8-y-old male donor), frontal cerebral cortex, and kidney (both from a 4-y-old male). In addition, DNA was extracted from one natural killer (NK) cell blood isolate (from an 8 y old male donor) and two additional full term placentas. DNA methylation was analyzed by MethylC-seq (Table S1). In contrast to the hypomethylation observed in all three placental samples (Fig. S1 *C* and *D*), methylation was globally higher in cerebral cortex (77.38%), cerebellum (75.73%), NK cells (78.97%), and kidney (76.80%). Furthermore, Fig. 1*A* shows that placenta was unique from other postnatal human tissues, exhibiting local methylation levels with sharp domain structures similar to PMDs previously characterized in some cell lines but dissimilar to the globally low methylation levels seen in adipose-derived stem cells (Fig. S1 *E* and *F*). Fig. 1*B* shows that the frequency distribution of local placental methylation levels is distinctly bimodal, with peaks of both partially methylated (about 45% methylated) and highly methylated (about 80% methylated) regions. To confirm that regions of low methylation are a consistent feature in placenta, we performed DNA methylation pyrosequencing of PMD and HMD regions in 10 additional full-term human placentas sampled similarly from the fetal side of the chorionic villi after removal of surface membranes (Fig. S1 *G* and *H* and Table S2). Placental samples were reproducibly distinct from other tissues in their lower methylation levels within PMDs but not HMDs. Intriguingly, data from the two additional placenta MethylC-seq samples suggest that much of the global differences in methylation between placentas occurs in the PMDs, not the HMDs (Fig. S1 *C* and *E*).

To objectively define PMD regions and boundaries, we performed a hidden Markov model analysis of the MethylC-seq data from all three placental samples. A representative region, the long arm of chromosome 21, is shown in Fig. S2*A* along with the hidden Markov model PMD predictions. Placental PMD locations are in Dataset S1. We found that placenta PMDs cover 37% of the autosomes, similar to the 41% coverage found in IMR90 cells. Placenta PMDs cover 3,815 genes, representing about 17% of the genes in the human genome. There was extensive overlap of PMDs between individuals, with a minimum pair-wise overlap between samples of 90.1% based on number of covered CpG sites (Fisher exact test: P value $< 2.2 \times 10^{-16}$; odds ratio: 875).

To determine whether PMDs can be observed with a non–sequencing-based genomic method, we examined additional placental samples using the Illumina Infinium 450K hybridization-based methylation platform. Because the arrays are biased toward coverage of promoters, CpG islands, and CpG island shores, which often have low methylation, we removed them from the Infinium data and separated the remaining CpG sites into our

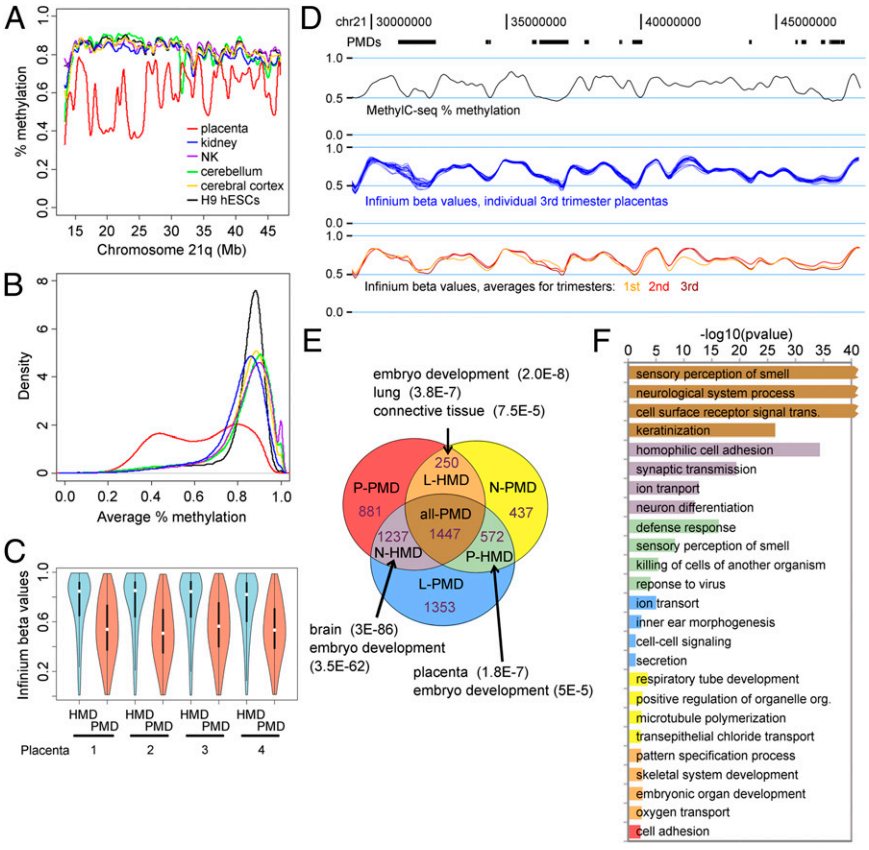

Fig. 1. Placenta has PMDs covering tissue-specific genes. (*A*) Methylation levels across the long arm of chromosome 21 in five noncultured human tissues and the H9 hESC line. Smoothing was done using a kernel smoother. (*B*) The distribution of average percent methylation across 20-kb windows tiling all autosomes. (*C*) Violin plots showing distribution of methylation levels from four different individuals in HMD and PMD regions from all autosomes on the Infinium 450K array. (*D*) Representative example on 21q of hidden Markov model-derived PMDs maps (top black bars) based on MethylC-seq data (black landscape plot). In comparison are Infinium 450K data from 21 different third-trimester placental samples (blue landscape plots) and the average of 5 first-trimester (yellow), 6 second-trimester (red), and 21 third-trimester (brown) placental samples. Promoters, CpG islands, and CpG island shores were removed from Infinium data before analysis. (*E*) Placental PMDs (upper left circle) were analyzed for overlap with previously described PMDs in neuronal cells (SH-SY5Y; upper right circle) and fetal lung fibroblast cells (IMR90; lower circle). These overlaps were used to define seven tissue-specific PMD subtypes: placenta-specific PMDs (P-PMD; red), neuronal-specific PMDs (N-PMD; yellow), lung-specific PMDs (L-PMD; blue), lung-specific HMDs (L-HMD; orange), neuronal-specific HMDs (N-HMD; purple), placenta-specific HMDs (P-HMD; green), and PMDs in all three tissues (all-PMD; brown). The number of genes in each domain type is shown. Tissues with higher expression of genes in L-HMDs, N-HMDs, and P-HMDs by DAVID analysis are diagrammed with arrows. These subdomains are predicted to have genes with functions specific to that tissue type. Benjamini significance values are shown. (*F*) GO biological process classifications for genes in each domain subtype using DAVID, color-coded as in Fig. 1*E*. "Sensory perception of "smell," "neurological system process," and "cell surface receptor signal transduction" had Benjamini P values of 1.2×10^{-265}, 4.0×10^{-148}, and 1.5×10^{-104}, respectively.

previously defined placental PMDs and HMDs. Clear differences in methylation could be detected in PMDs and HMDs despite the Infinium 450K array's biased probe representation over CpG islands and poor coverage over PMDs (Fig. S2*B*). Genome-wide methylation analysis of placental PMDs and HMDs in four representative third trimester placentas (30) showed consistently low methylation in PMDs with Infinium β values of 0.4–0.7 (Fig. 1*C*).

We next asked whether placental PMD patterns changed with gestational age. Placental samples from first, second, and third trimesters were analyzed on the Illumina 450K arrays and compared with the MethylC-seq data on chromosome 21 (Fig. 1*D*). The pattern of methylation levels across the chromosome in both MethylC-seq and Illumina 450K corresponded well. Importantly, there was little variation in placental methylation landscape across all three trimesters with average chromosome 21 β values ranging from 0.62 to 0.71 and a minimum pair-wise correlation between placentas of 0.78. This suggests that PMDs are a general feature of the placenta methylome that are maintained throughout gestational stages.

Because LINE-1 elements are often found to be hypomethylated in cancer (31) and placenta (12, 32), we investigated whether the low methylation in PMDs could be explained by enrichment of hypomethylated LINE-1 elements. However, analysis of MethylC-seq placenta data showed that LINE-1 elements were only slightly more highly represented in PMDs and only comprised 21% of the PMD length (Fig. S2 *C–E*). Moreover, within both PMDs and HMDs there was no difference in methylation levels between LINE-1 elements and non-LINE-1–containing sequence (Fig. S2*F*). In fact, LINE-1 methylation levels mirror the average genome methylation levels observed by MethylC-Seq (Fig. S2*G*).

We previously found in SH-SY5Y and IMR90 cells that genes within tissue-specific PMDs were enriched for tissue-specific functions. Now, by comparing the overlap of genes within PMDs of all three tissue sources [placenta (P), neuron (N), lung (L) fibroblast], seven different tissue-specific PMD subtypes were defined (Fig. 1*E* and Dataset S2). Genes were most numerous in the PMD subtypes defined as all-PMD (PMDs in all three tissues), L-PMDs (PMD in IMR90 but HMD in placenta and SH-SY5Y), and N-HMDs (PMD in IMR90 and placenta but HMD in SH-SY5Y). Consistent with our previous results, gene ontology (GO) analysis showed that N-HMDs were enriched for neuronal genes and L-HMDs were enriched for respiratory tube development genes (Fig. 1*F* and Dataset S3). Importantly, genes in placenta-specific HMDs (P-HMDs) were significantly more likely to have defense response functions. To determine whether genes in PMD subtypes had the expected tissue-specific expression, we took the genes that were most likely to have functions relevant to only one tissue (P-HMDs, N-HMDs, and L-HMDs) and submitted them to DAVID (33) to determine which tissue they were most likely expressed in based on microarray data. All three tissues were correctly identified based on the gene lists within P-HMDs, N-HMDs, and L-HMDs (Fig. 1*E*).

To determine whether genes in placental PMDs are repressed in placenta, we performed RNA-seq on the same placental sample (Table S3). The results confirmed that genes in PMDs (Fig. 2*A*) and with low gene body methylation (Fig. 2*B*) had lower gene expression than those that were highly methylated, similar to the relationship observed in IMR90 and SH-SY5Y cells (5, 6). Thus, the general biological properties of PMDs observed in tissue culture cells also apply to human placental tissue. In addition, PMDs were easily detected in RNA-seq reads genome-wide as large domains with lower transcript levels (Fig. 2*C*).

Genes Within Placental PMDs Show Hypomethylation of Gene Bodies but Hypermethylation of CpG Islands Compared with Those Within HMDs. Because most promoter associated CpG islands in the human genome are characterized by very low levels of DNA methylation compared with the rest of the genome, we used MethylC-seq data to determine whether this was also true for genes within PMDs. We defined promoters as regions −1000 to +100 bp from a transcription start site and CpG islands were those annotated by the Santa Cruz Genome Browser. As expected, the median gene body methylation (omitting CpG islands) in placental PMDs and HMDs is 48.2% and 79.3%, respectively (Fig. 3*A*). Promoters and CpG islands have much lower methylation than other regions in both PMDs and HMDs. However, promoters show 6% more methylation in PMD genes compared with HMD genes (Fig. 3*B* and Fig. S3*A*). Looking only at promoters with CpG islands, again, there is 4% more methylation in PMD genes compared with HMD genes (Fig. 3*C* and Fig. S3 *B*, *D*, and *E*). In contrast to promoter CpG islands, gene body CpG islands within PMDs follow the dominant overall PMD methylation levels, showing lower levels of methylation within PMDs compared with gene body CpG islands within HMDs (Fig. 3*D* and Fig. S3 *C*, *F*, and *G*).

Because the "shores" of CpG islands, defined as 2-kb upstream and downstream of promoter CpG islands (34), have been described as sites of tissue-specific differentially methylated regions (35), we also asked whether there were differences in methylation in PMDs and HMDs at promoter CpG island shores. In both PMDs and HMDs, the distinct patterns of CpG island methylation returns to gene body levels 1–2 kb away from the CpG island (Fig.

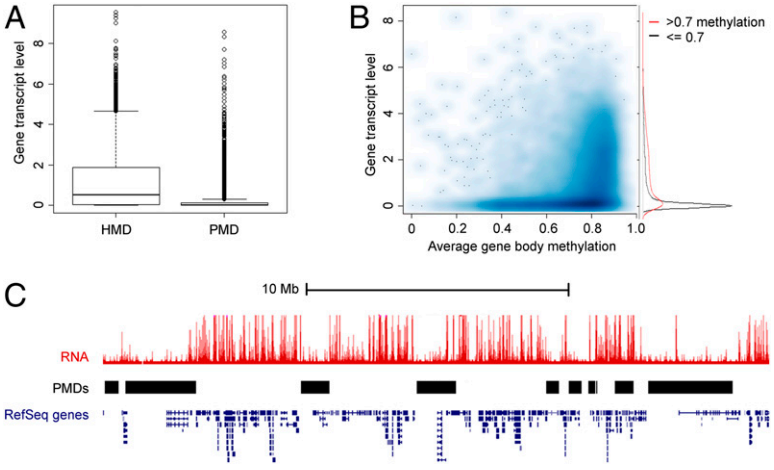

Fig. 2. Genes in PMDs have lower transcript levels. (*A*) Differences in gene expression between genes in PMDs and HMDs in placenta. Transcript levels are shown as log (FPKM + 1). Only RNA-seq reads that mapped to known transcripts were used for FPKM analysis. (*B*) Average gene body methylation versus gene expression in placenta. Promoters and CpG islands were removed before computing the average gene body methylation. The histograms to the right show the expression distributions for genes with greater than (red) and less than (black) 70% average gene body methylation. (*C*) Genomic view of placental data on chromosome 7 showing low levels of transcription within PMDs. The RNA library was not poly-A–selected and reads were mapped to the entire genome using Bowtie.

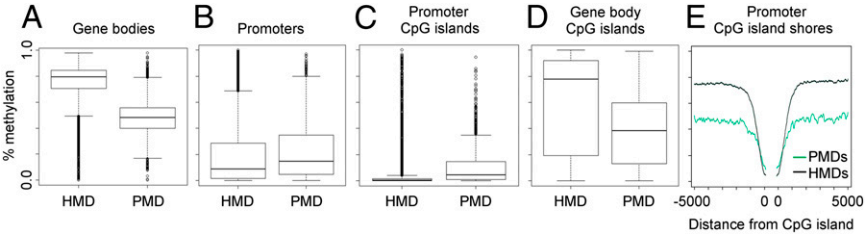

Fig. 3. Regulatory elements within PMDs have distinct levels of methylation. DNA methylation analysis for gene regulatory elements within placental PMDs and HMDs. (*A–D*) Levels of placental DNA methylation within gene bodies (*A*), promoters (*B*), promoter CpG islands (*C*), and gene body CpG islands (*D*). All four showed significant differences between PMDs and HMDs (Wilcoxon rank sum test P values $< 8 \times 10^{-10}$). For gene body methylation analysis, CpG islands and promoters were first removed. (*E*) DNA methylation levels on the shores of promoter CpG islands.

3*E*). Separating PMDs and HMDs according to their tissue specificity defined in Fig. 1*E*, we found that promoter CpG island shores in placental PMDs (all-PMDs, P-PMDs, N-HMDs, and L-HMDs) have consistently lower slopes of percent methylation transition from CpG island shore to island (Fig. S4 *A* and *B*). A similar analysis of promoter CpG island shores in SH-SY5Y PMDs gave comparable results (Fig. S4 *C–F*).

Polycomb-Regulated Regions Have Higher Methylation in Placental HMDs Than in PMDs. To compare DNA methylation in placental PMDs and polycomb-regulated regions, we first defined polycomb-regulated regions as those bound by both RING1B and EZH2 in H9 hESCs (25). These polycomb-regulated regions tend to be shorter than PMDs, the longest being 134-kb over the HOXC cluster, and, in all, cover about 0.37% of the human genome. They overlapped 783 genes, most of which are transcription factors that regulate development. The most significant GO terms were regulation of transcription (9.1×10^{-92}) and embryonic morphogenesis (7.0×10^{-74}).

MethylC-seq analysis of multiple human tissues found that regions of polycomb-associated hypomethylation occur in most tissues and cell lines, including H9 human embryonic stem cells (Fig. 4). Fig. 4*A* shows the *DLX5/6* locus, which is transcriptionally active in placenta but not in the other tissues examined. In nonplacental tissues, low methylation is observed across the entire polycomb-regulated region. In placenta, however, the *DLX5/6* locus is within an HMD. In contrast, the *MSX1* locus is in a PMD in placenta and transcriptionally inactive (Fig. 4*B*). Methylation levels in the surrounding PMD encompassing *MSX1* are low, but not as low as in the polycomb-regulated region.

Globally, polycomb-regulated regions have distinct methylation patterns when found within PMDs versus HMDs in placenta (Fig. 4*C*). Polycomb-regulated regions have much lower levels of methylation when found within PMDs compared with HMDs. In addition, in both PMDs and HMDs, polycomb-regulated regions have lower levels of methylation than the surrounding genomic sequence. These data suggest that although the hypomethylation in polycomb-regulated regions is both greater than and mechanistically distinct from hypomethylation of PMDs, these regions still reflect the local methylation properties defined by the larger scale PMD/HMD landscape.

We next asked whether methylation levels in polycomb-regulated regions were similar among tissues. Except for placenta, all tissues and the hESCs had similar levels of methylation within polycomb-regulated regions (Fig. 4*D*) and the CpG islands within them (Fig. S4*G*). However, placenta showed higher levels of methylation in both polycomb-regulated regions and their CpG islands. Comparing Fig. 4 *C* and *D*, it appears that the higher average levels of methylation in placenta polycomb regions compared with other tissues is largely attributable to the HMD polycomb regions because the placental PMD polycomb regions (Fig. 4*C*, red) have a very similar distribution to that of the polycomb regions in other tissues (Fig. 4*D*). This is consistent with polycomb-regulated genes in HMDs showing higher levels of expression than those in PMDs and the association observed between PMD location and gene repression (Fig. S4*H*). Lastly, we investigated the differences in domain size represented by PMDs versus polycomb regions (Fig. 4*E*), demonstrating that PMDs are distinctly larger than polycomb regions. This result was highly robust to the hidden Markov model transition probabilities used (Fig S4*I*).

Discussion

Here, we performed MethylC-seq in full-term human placenta, discovering a normal human tissue showing clear evidence of PMDs and identifying several unique properties of the placental methylome. Using Illumina Infinium 450K arrays, we also found that PMD patterns and methylation levels are stable during the three trimesters of placenta development. In contrast to the high interplacenta variability previously seen using an ELISA method (19), we find relatively little variability in global methylation patterns as determined by Infinium arrays, pyrosequencing, and MethylC-seq. Similar to cultured human cells with PMDs, genes within PMDs in placenta are repressed and have tissue-specific functions. Because P-HMD genes are found within PMDs in IMR90 and SH-SY5Y cells but are highly methylated in placenta, they would be expected to have placenta-specific functions and expression. Notably, P-HMDs are enriched for genes with functions in defense response, a function pertinent to the unique interface of the maternal and fetal blood supplies that occurs in placenta (22). Interestingly, promoter CpG islands show higher methylation for genes within PMDs, despite their presence within a domain of overall low methylation. This is similar to the epigenetic profile seen in some cancers where there is global hypomethylation but hypermethylation at promoters. Polycomb-regulated regions, previously referred to as "methylation deserts" (29) because of their hypomethylation in a variety of tissues, are distinct from PMDs in size and uniquely methylated in placenta compared with other tissues with no PMDs.

Our results and those of others therefore suggest that there are distinct patterns and mechanisms leading to large-scale hypomethylation in human development and disease. From the few "hypomethylated" human methylomes sequenced thus far, it is becoming increasingly clear that distinctions need to be made between those with PMDs and those with randomly distributed global hypomethylation. Whereas human adipose-derived stem cells (3) and mouse maturing red blood cells (4) appear to have lower methylation levels genome-wide without PMDs, other cell lines and tissues such as human placenta have normal methylation levels over most of the genome but distinct hypomethylation within PMDs that cover 15–40% of the genome. A third type of genomic hypomethylation pattern occurs over polycomb-regulated genes that cover only 1% of the genome and are a distinct (but interrelated) phenomenon from PMDs in placenta.

It is also becoming clear that analysis of methylation at gene features such as promoters, CpG islands, and CpG island shores

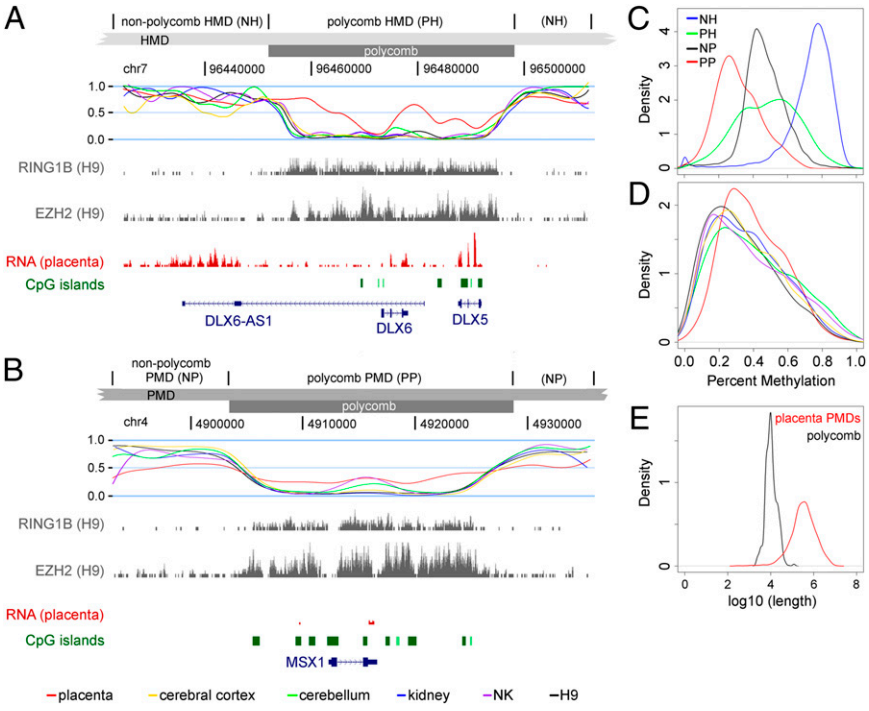

Fig. 4. Polycomb-regulated regions have unique methylation patterns in PMDs and HMDs. (*A* and *B*) DNA methylation within the polycomb-regulated *DLX5/6* (*A*) and *MSX1* (*B*) loci for six different tissues. The RNA-seq track is from the non-poly-A selected placental library with reads mapped to the entire genome using Bowtie. RING1B and EZH2 ChIP-seq data tracks are from Ku et al. (25). The hidden Markov model analysis showed entirely within a placental HMD (*A*) and entirely within a placental PMD (*B*). (*C*) Comparison of placenta methylation levels in nonpolycomb HMDs (NH), polycomb HMDs (PH), nonpolycomb PMDs (NP), and polycomb PMDs (PP). For each group, CpG islands were removed before assessing average percent methylation. For nonpolycomb regions, genomic DNA was divided into ≤100-kb subregions for better comparison with polycomb regions. (*D*) Comparison of non-CpG island methylation levels within polycomb regions between six different tissues. Placenta (red) is distinct from other tissues in methylation of polycomb-regulated regions. (*E*) Distribution of the lengths of polycomb-regulated regions and PMDs.

must take into account both global and local methylation context for that tissue, especially when comparing normal and cancer tissues. Recent studies have shown that some colon (7, 8) and breast cancers (9, 10) have PMDs that cover large portions of the genome. In colon cancer, Berman and coworkers found that hypermethylated CpG islands tended to occur in colon cancer PMDs (8), suggesting a link between the global hypomethylation and CpG island hypermethylation observed in some cancers (36, 37). Our data in normal human placenta also show higher levels of DNA methylation in promoter CpG islands within PMDs compared with HMDs, suggesting that promoter hypermethylation compared with other tissues may not be specific to cancer.

Although placenta shows clear evidence of PMDs, the question remains whether other tissues, possibly at specific stages of development, may also have PMDs and what these PMDs may mean for gene regulation. Interestingly, it was found that cancer PMD regions in colon and breast also showed slightly reduced methylation in the normal tissue/cell line used for comparison, although the reduced levels of methylation were weak and didn't qualify as full PMDs (8, 10). Therefore, it is possible that the slightly reduced methylation levels in normal tissue are remnants of PMDs earlier in the tissue's development. Another possibility is that, because of cellular heterogeneity, PMDs in normal colon and breast are difficult to detect because they are limited to a small subset of cells. Alternatively, PMDs in the cancer tissue may be an exacerbation of lagging DNA methylation at late replicating regions caused by the accelerated cell cycle in cancers (10). A final possibility is that placenta is the only normal tissue with PMDs and that some cancers may activate placental-specific programming. Supporting this hypothesis is the fact that extravillous trophoblasts in the placenta are able to migrate, invade, and remodel the maternal decidua in a manner similar to some cancers and that many tumor suppressor genes and oncogenes are important for normal placental development (22). Regardless, these large PMDs correspond to unique genomic landmarks identifying domains associated with developmentally regulated, tissue-specific gene repression programs.

We provide a comprehensive map of PMDs in the human full-term placenta that will be important for future studies of infant growth rate, preeclampsia, and preterm delivery. We have also demonstrated the detectability of PMDs using the Illumina Infinium 450K platform, which could help in the interpretation of methylation differences observed in other Infinium 450K studies, as well as improving PMD probe coverage in future array-based platforms. Lastly, because PMDs contain many neuronal developmental genes, including many genes implicated in autism (6), our results could be useful for future studies to determine whether epigenetic dysregulation of autism genes can be detected at birth.

Materials and Methods

MethylC-seq. MethylC-seq data from H9 hESCs was published previously (38). Full-term human placental samples were obtained from normal Cesarean sections. Chorionic villous tissue was obtained from the fetal side of the placenta. NK cells were isolated from a male donor by $CD56^+$ bead sorting as described previously (39). Human cerebral cortex, cerebellum, and kidney samples were obtained from the NICHD Brain and Tissue Bank for Developmental Disorders at the University of Maryland. Tissue DNA was purified using the Qiagen Puregene kit. MethylC-seq libraries were made as described previously (6). Briefly, the genomic DNA was sonicated to ~300 bp, and methylated Illumina adapters were ligated to the ends. The library was bisulfite converted, amplified for 12 cycles, and sequenced on either an Illumina HiSeq or GAII. Reads were mapped to the hg18 version of the human genome using BS Seeker (40) and only one read per genomic position was kept to prevent clonal PCR amplification biases. CpG site methylation data were combined from both DNA strands. After masking out CpG islands, a two-state hidden Markov model was trained as in ref. 6 using StochHMM (*SI Materials and Methods*, Fig. S5, and Table S4).

Methylation Pyrosequencing. Samples were taken from six different locations in ten full-term placentas (Table S2). Twenty-four random samples were used for blinded analysis. Genomic DNA was isolated and bisulfite converted as above, PCR-amplified for 42 cycles using Taq polymerase (Invitrogen), and run on a PyroMark Q24. Primer sequences are provided in Table S5. Human LINE-1 pyrosequencing primers were from Qiagen.

Illumina Infinium 450K Array Analysis. Thirty-six placental samples [5 first-trimester (8–12 wk), 10 second-trimester (15–24 wk), and 21 third-trimester (30–40 wk)] were analyzed on the Illumina HumanMethylation450 BeadChip (Illumina). At least two sites were taken from each placenta and the extracted

GENETICS

DNA was combined in equal amounts to correct for intraplacental variability. DNA was extracted using standard protocols, bisulfite-converted using the EZ DNA Methylation Kit (Zymo Research), and hybridized to arrays following the manufacturer's protocol. Arrays were scanned by a HiScan 2000 or iScan (Illumina). Background subtraction and initial processing was performed using Genome Studio 2011 (Illumina). Probes targeting a CpG with a SNP in the C or G were removed from analysis. Valid probes were color channel-corrected, separated into type I and type II probes, and normalized by SWAN (41). M values were converted in to β values for genome-wide analysis (42). Promoters, CpG islands, and CpG island shores were removed before PMD analysis.

RNA-seq. Using the same two placenta replicate samples used for MethylC-seq, RNA was extracted using the NuGEN Ovation RNA-Seq System. Indexed adapters were added using the NuGEN Encore NGS Library System I. The two libraries were combined and sequenced on a single Illumina HiSeq lane. Reads were mapped to the hg18 version of the genome using TopHat (43). Cufflinks was used to obtain FPKM scores, omitting reads that did not align to known transcripts.

Identifying Polycomb-Regulated Regions. Using ChIP-seq data for RING1B and EZH2 from H9 hESCs (25), genomic regions were identified that bound RING1B (>20 mapped reads per 5-kb window) and EZH2 (>50 mapped reads per 5-kb window) individually over at least 5.5 kb. Polycomb-regulated regions were then defined as those where RING1B and EZH2 overlapped for at least 2 kb.

ACKNOWLEDGMENTS. We thank the laboratory of W.P.R. for placental collection and array processing, Amanda Enstrom for help the NK cell sample, the laboratory of J.M.L. for helpful comments, and Dr. Gordon Douglas for critical reading of the manuscript. This work was supported by National Institutes of Health (NIH) Grants R01HD041462 and R01ES021707 (to J.M.L), Department of Defense Grant AR110194 (to J.M.L), and Canadian Institutes for Health Research Grant FRN 119402 (to W.P.R.).

1. Ehrlich M, et al. (1982) Amount and distribution of 5-methylcytosine in human DNA from different types of tissues of cells. *Nucleic Acids Res* 10(8):2709–2721.
2. Gama-Sosa MA, et al. (1983) Tissue-specific differences in DNA methylation in various mammals. *Biochim Biophys Acta* 740(2):212–219.
3. Lister R, et al. (2011) Hotspots of aberrant epigenomic reprogramming in human induced pluripotent stem cells. *Nature* 471(7336):68–73.
4. Shearstone JR, et al. (2011) Global DNA demethylation during mouse erythropoiesis in vivo. *Science* 334(6057):799–802.
5. Lister R, et al. (2009) Human DNA methylomes at base resolution show widespread epigenomic differences. *Nature* 462(7271):315–322.
6. Schroeder DI, Lott P, Korf I, LaSalle JM (2011) Large-scale methylation domains mark a functional subset of neuronally expressed genes. *Genome Res* 21(10):1583–1591.
7. Hansen KD, et al. (2011) Increased methylation variation in epigenetic domains across cancer types. *Nat Genet* 43(8):768–775.
8. Berman BP, et al. (2012) Regions of focal DNA hypermethylation and long-range hypomethylation in colorectal cancer coincide with nuclear lamina-associated domains. *Nat Genet* 44(1):40–46.
9. Shann Y-J, et al. (2008) Genome-wide mapping and characterization of hypomethylated sites in human tissues and breast cancer cell lines. *Genome Res* 18(5):791–801.
10. Hon GC, et al. (2012) Global DNA hypomethylation coupled to repressive chromatin domain formation and gene silencing in breast cancer. *Genome Res* 22(2):246–258.
11. Fuke C, et al. (2004) Age related changes in 5-methylcytosine content in human peripheral leukocytes and placentas: An HPLC-based study. *Ann Hum Genet* 68(Pt 3): 196–204.
12. Cotton AM, et al. (2009) Inactive X chromosome-specific reduction in placental DNA methylation. *Hum Mol Genet* 18(19):3544–3552.
13. Grigoriu A, et al. (2011) Cell specific patterns of methylation in the human placenta. *Epigenetics* 6(3):368–379.
14. Novakovic B, Saffery R (2010) DNA methylation profiling highlights the unique nature of the human placental epigenome. *Epigenomics* 2(5):627–638.
15. Chu T, et al. (2011) Structural and regulatory characterization of the placental epigenome at its maternal interface. *PLoS ONE* 6(2):e14723.
16. Aran D, Toperoff G, Rosenberg M, Hellman A (2011) Replication timing-related and gene body-specific methylation of active human genes. *Hum Mol Genet* 20(4):670–680.
17. Yuen RK, Peñaherrera MS, von Dadelszen P, McFadden DE, Robinson WP (2010) DNA methylation profiling of human placentas reveals promoter hypomethylation of multiple genes in early-onset preeclampsia. *Eur J Hum Genet* 18(9):1006–1012.
18. Banister CE, et al. (2011) Infant growth restriction is associated with distinct patterns of DNA methylation in human placentas. *Epigenetics* 6(7):920–927.
19. Chavan-Gautam P, et al. (2011) Gestation-dependent changes in human placental global DNA methylation levels. *Mol Reprod Dev* 78(3):150.
20. Kulkarni A, Chavan-Gautam P, Mehendale S, Yadav H, Joshi S (2011) Global DNA methylation patterns in placenta and its association with maternal hypertension in pre-eclampsia. *DNA Cell Biol* 30(2):79–84.
21. Lambertini L, et al. (2011) Differential methylation of imprinted genes in growth-restricted placentas. *Reprod Sci* 18(11):1111–1117.
22. Novakovic B, Saffery R (2012) The ever growing complexity of placental epigenetics - role in adverse pregnancy outcomes and fetal programming. *Placenta* 33(12):959–970.
23. Lynch MD, et al. (2012) An interspecies analysis reveals a key role for unmethylated CpG dinucleotides in vertebrate Polycomb complex recruitment. *EMBO J* 31(2):317–329.
24. Mendenhall EM, et al. (2010) GC-rich sequence elements recruit PRC2 in mammalian ES cells. *PLoS Genet* 6(12):e1001244.
25. Ku M, et al. (2008) Genomewide analysis of PRC1 and PRC2 occupancy identifies two classes of bivalent domains. *PLoS Genet* 4(10):e1000242.
26. Tanay A, O'Donnell AH, Damelin M, Bestor TH (2007) Hyperconserved CpG domains underlie Polycomb-binding sites. *Proc Natl Acad Sci USA* 104(13):5521–5526.
27. Branciamore S, Chen Z-X, Riggs AD, Rodin SN (2010) CpG island clusters and pro-epigenetic selection for CpGs in protein-coding exons of HOX and other transcription factors. *Proc Natl Acad Sci USA* 107(35):15485–15490.
28. Orlando DA, Guenther MG, Frampton GM, Young RA (2012) CpG island structure and trithorax/polycomb chromatin domains in human cells. *Genomics* 100(5):320–326.
29. Li J, et al. (2012) Genomic hypomethylation in the human germline associates with selective structural mutability in the human genome. *PLoS Genet* 8(5):e1002692.
30. Price EM, et al. (2013) Additional annotation enhances potential for biologically-relevant analysis of the Illumina Infinium HumanMethylation450 BeadChip array. *Epigenetics Chromatin* 6(1):4.
31. Pavicic W, Joensuu EI, Nieminen T, Peltomäki P (2012) LINE-1 hypomethylation in familial and sporadic cancer. *J Mol Med (Berl)* 90(7):827–835.
32. Price EM, et al. (2012) Different measures of "genome-wide" DNA methylation exhibit unique properties in placental and somatic tissues. *Epigenetics* 7(6):652–663.
33. Huang W, Sherman BT, Lempicki RA (2009) Bioinformatics enrichment tools: Paths toward the comprehensive functional analysis of large gene lists. *Nucleic Acids Res* 37(1):1–13.
34. Irizarry RA, et al. (2009) The human colon cancer methylome shows similar hypo- and hypermethylation at conserved tissue-specific CpG island shores. *Nat Genet* 41(2): 178–186.
35. Ji H, et al. (2010) Comprehensive methylome map of lineage commitment from haematopoietic progenitors. *Nature* 467(7313):338–342.
36. Jones PA, Baylin SB (2007) The epigenomics of cancer. *Cell* 128(4):683–692.
37. Ehrlich M (2009) DNA hypomethylation in cancer cells. *Epigenomics* 1(2):239–259.
38. Martins-Taylor K, Schroeder DI, Lasalle JM, Lalande M, Xu R-H (2012) Role of DNMT3B in the regulation of early neural and neural crest specifiers. *Epigenetics* 7(1):71–82.
39. Enstrom AM, et al. (2009) Altered gene expression and function of peripheral blood natural killer cells in children with autism. *Brain Behav Immun* 23(1):124–133.
40. Chen P-Y, Cokus SJ, Pellegrini M (2010) BS Seeker: Precise mapping for bisulfite sequencing. *BMC Bioinformatics* 11:203.
41. Maksimovic J, Gordon L, Oshlack A (2012) SWAN: Subset-quantile within array normalization for illumina infinium HumanMethylation450 BeadChips. *Genome Biol* 13(6):R44.
42. Du P, et al. (2010) Comparison of Beta-value and M-value methods for quantifying methylation levels by microarray analysis. *BMC Bioinformatics* 11:587.
43. Trapnell C, et al. (2012) Differential gene and transcript expression analysis of RNA-seq experiments with TopHat and Cufflinks. *Nat Protoc* 7(3):562–578.